

Scaling properties of background- and chiral-magnetically-driven charge separation: evidence for detection of the chiral magnetic effect in heavy ion collisions

Roy Lacey^{1,*}

¹Depts. of Chemistry & Physics, Stony Brook University, Stony Brook, New York 11794, USA

Abstract. The scaling properties of the $R_{\Psi_2}(\Delta S)$ correlator and the $\Delta\gamma$ correlator are used to investigate a possible chiral-magnetically-driven (CME) charge separation in p +Au, d +Au, Ru+Ru, Zr+Zr, and Au+Au collisions at $\sqrt{s_{\text{NN}}} = 200$ GeV, and in p +Pb ($\sqrt{s_{\text{NN}}} = 5.02$ TeV) and Pb+Pb collisions at $\sqrt{s_{\text{NN}}} = 5.02$ and 2.76 TeV. The results for p +Au, d +Au, p +Pb, and Pb+Pb collisions, show the $1/N_{\text{ch}}$ scaling for background-driven charge separation. However, the results for Au+Au, Ru+Ru, and Zr+Zr collisions show scaling violations which indicate a CME contribution in the presence of a large background. In mid-central collisions, the CME accounts for approximately 27% of the signal + background in Au+Au and roughly a factor of two smaller for Ru+Ru and Zr+Zr, which show similar magnitudes.

Metastable domains of gluon fields with non-trivial topological configurations can form in the magnetized chiral relativistic quark-gluon plasma (QGP) [1] produced in collisions at RHIC and the LHC. The colliding ions generate the magnetic field (\vec{B}) at early times [2]. The interaction of chiral quarks with the gluon fields can drive a chiral imbalance resulting in an electric current $\vec{J}_V = \frac{N_c e \vec{B}}{2\pi^2} \mu_A$, along the \vec{B} -field, i.e., roughly perpendicular to the reaction plane; N_c is the color factor, and μ_A is the axial chemical potential that quantifies the imbalance between right- and left-handed quarks. The resulting final-state charge separation, termed the chiral magnetic effect (CME) [1], is of great experimental and theoretical interest. However, its experimental characterization has been hampered by significant background.

The charge separation can be quantified via the P -odd sine term a_1 , in the Fourier decomposition of the charged-particle azimuthal distribution [3]:

$$\frac{dN_{\text{ch}}}{d\phi} \propto 1 + 2 \sum_n (v_n \cos(n\Delta\phi) + a_n \sin(n\Delta\phi) + \dots) \quad (1)$$

where $\Delta\phi = \phi - \Psi_{\text{RP}}$ gives the particle azimuthal angle with respect to the reaction plane (RP) angle, and v_n and a_n denote the coefficients of the P -even and P -odd Fourier terms, respectively. A direct measurement of a_1 , is not possible due to the strict global \mathcal{P} and \mathcal{CP} symmetry of QCD. However, their fluctuation and/or variance $\tilde{a}_1 = \langle a_1^2 \rangle^{1/2}$ can be measured with charge-sensitive correlators such as the γ -correlator [3] and the $R_{\Psi_2}(\Delta S)$ correlator [4].

The γ -correlator measures charge separation as: $\gamma_{\alpha\beta} = \langle \cos(\phi_\alpha + \phi_\beta - 2\Psi_2) \rangle$, $\Delta\gamma = \gamma_{0S} - \gamma_{SS}$, where Ψ_2 is the azimuthal angle of the 2nd-order event plane which fluctuates

*e-mail: Roy.Lacey@Stonybrook.edu

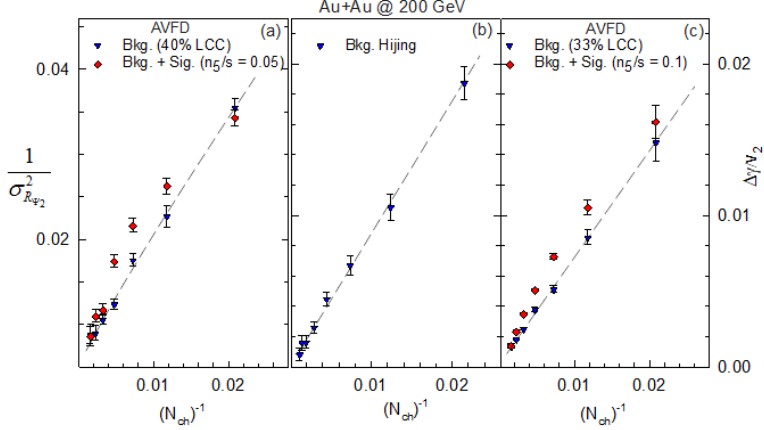


Figure 1. $\sigma_{R_{\Psi_2}}^{-2}$ vs. $1/N_{\text{ch}}$ (a) and $\Delta\gamma/v_2$ vs. $1/N_{\text{ch}}$ (b) and (c) for simulated Au+Au collisions at $\sqrt{s_{\text{NN}}} = 200$ GeV. The results for $\sigma_{R_{\Psi_2}}^{-2}$ and $\Delta\gamma/v_2$ from the AVFD model are shown for background and for signal + background as indicated. The Hijing model results are only shown for the background. The dashed lines represent linear fits to the background values.

about the RP, ϕ denote the particle azimuthal emission angles, α, β denote the electric charge (+) or (-) and SS and OS represent same-sign (++, --) and opposite-sign (+-) charges. Measurements of the quotient $\Delta\gamma/v_2$ with the 2nd-order anisotropy coefficient v_2 , are usually employed to aid quantification of the background-driven charge separation.

The $R_{\Psi_2}(\Delta S)$ correlator measures charge separation relative to Ψ_2 via the ratio: $R_{\Psi_2}(\Delta S) = C_{\Psi_2}(\Delta S)/C_{\Psi_2}^{\perp}(\Delta S)$, where $C_{\Psi_2}(\Delta S)$ and $C_{\Psi_2}^{\perp}(\Delta S)$ are correlation functions that quantify charge separation ΔS , approximately parallel and perpendicular (respectively) to the \vec{B} -field. The charge-shuffling procedure used to construct the correlation functions ensures identical properties for their numerator and denominator, except for the charge-dependent correlations, which are of interest [4]. $C_{\Psi_2}(\Delta S)$ measures both CME- and background-driven charge separation while $C_{\Psi_2}^{\perp}(\Delta S)$ measures only the background. After correcting the $R_{\Psi_2}(\Delta S)$ distributions for the effects of particle-number fluctuations and the event-plane resolution, their inverse variance $\sigma_{R_{\Psi_2}}^{-2}$ are used to quantify the charge separation [4].

In this work, we use model simulations to chart the scaling properties of $\sigma_{R_{\Psi_2}}^{-2}$ and $\Delta\gamma/v_2$ for the background and signal + background, respectively, in A+A collisions. We then leverage these scaling properties to identify and characterize a possible CME-driven charge separation using previously published data for p +Au, d +Au, Ru+Ru, Zr+Zr and Au+Au collisions at RHIC [5–10], and p +Pb and Pb+Pb collisions at the LHC [11–14].

Figure 1 shows the results for $\sigma_{R_{\Psi_2}}^{-2}$ and $\Delta\gamma/v_2$ obtained with the AVFD and Hijing models for Au+Au collisions. Note that these models emphasize different sources for the charge-dependent non-flow background. The AVFD model also allows input values for the initial axial charge density n_5/s and the degree of local charge conservation (LCC) that regulate the magnitude of the CME- and background-driven charge separation. The solid triangles in Fig. 1 show that the background [for both models] scales as $1/N_{\text{ch}}$ – the expected trend for the charge-dependent non-flow correlations. By contrast, the signal (Sig.) + background values (solid diamonds) indicate positive deviations from the background scaling [16, 17]. This dependence can be represented as; $\Delta\gamma/v_2 = a + b/(N_{\text{ch}})^{1-c}$, and $\sigma_{R_{\Psi_2}}^{-2} = a' + b'/(N_{\text{ch}})^{1-c'}$, for the small values of n_5/s indicated in Fig. 1. Here, a, b and c are parameters; c characterizes

the degree of the scaling violation and the magnitude of the CME; for $c \sim 0$ the $1/N_{\text{ch}}$ scaling for the background is retrieved, as demonstrated for $\sigma_{R\psi_2}^{-2}$ and $\Delta\gamma/v_2$ with the AVFD model in Fig. 1.

The scaling violation for $\sigma_{R\psi_2}^{-2}$ and $\Delta\gamma/v_2$ (Figs. 1 (a) and (c)) gives a direct signature of the CME-driven contributions to the charge separation. It can be quantified via $c > 0$ and the fractions: $f_{\text{CME}}^{\Delta\gamma} = [\Delta\gamma/v_2(\text{Sig.} + \text{Bkg.}) - \Delta\gamma/v_2(\text{Bkg.})]/[\Delta\gamma/v_2(\text{Sig.} + \text{Bkg.})]$, $f_{\text{CME}}^R = [\sigma_{R\psi_2}^{-2}(\text{Sig.} + \text{Bkg.}) - \sigma_{R\psi_2}^{-2}(\text{Bkg.})]/[\sigma_{R\psi_2}^{-2}(\text{Sig.} + \text{Bkg.})]$. The scaling patterns in Fig. 1 suggest that the observation of $1/N_{\text{ch}}$ scaling for the experimental $\sigma_{R\psi_2}^{-2}$ and $\Delta\gamma/v_2$ measurements would strongly indicate background-driven charge separation with little room for a CME contribution. However, observing a violation of this $1/N_{\text{ch}}$ scaling would indicate the CME-driven contribution. Figs. 1 (a) and (c) also indicate comparable background and signal + background $\sigma_{R\psi_2}^{-2}$ and $\Delta\gamma/v_2$ values in central and peripheral collisions, suggesting that the background dominates over that of the CME-driven contributions in these collisions. This trend for the background is consistent with the reduction of \vec{B} in central collisions and the enhanced de-correlation between the event plane and the \vec{B} -field in peripheral collisions.

Since the background dominates in central and peripheral collisions, the $\sigma_{R\psi_2}^{-2}$ and $\Delta\gamma/v_2$ measurements for these collisions can be leveraged with $1/N_{\text{ch}}$ scaling to obtain a quantitative estimate of the background over the entire centrality span (cf. Fig. 1). Here, an important proviso is to experimentally establish that the background in $p(d)+A$ and $A+A$ collisions scale as $1/N_{\text{ch}}$ over the full centrality span.

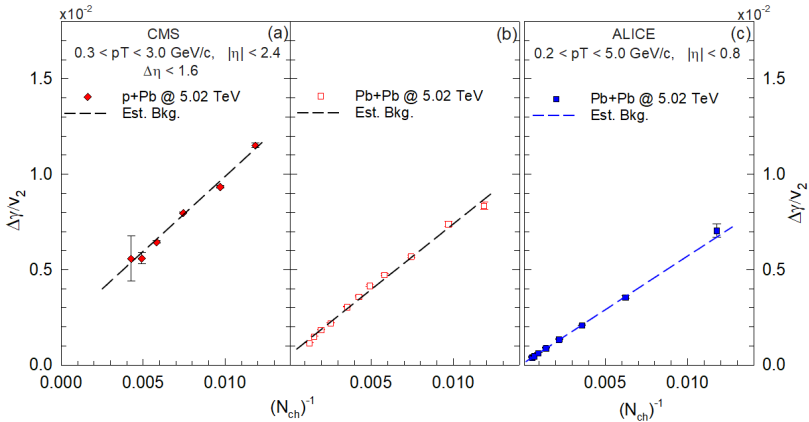


Figure 2. $\Delta\gamma/v_2$ vs. $1/N_{\text{ch}}$ for $p+Pb$ (a) and $Pb+Pb$ [(c) and (d)] collisions at $\sqrt{s_{\text{NN}}} = 5.02$ TeV. The dashed lines indicate an estimate of the background. The data are taken from Refs. [12, 13, 15].

The v_2 and $\Delta\gamma$ values reported for $p+Au$, $d+Au$, $Ru+Ru$, $Zr+Zr$ and $Au+Au$ collisions at RHIC [5–10], and $p+Pb$ and $Pb+Pb$ collisions at the LHC [12–15] were used to investigate the scaling properties of $\Delta\gamma/v_2$. Fig. 2 shows the results for $p+Pb$ and $Pb+Pb$ collisions at $\sqrt{s_{\text{NN}}} = 5.02$ TeV. They indicate that $\Delta\gamma/v_2$ essentially scales as $1/N_{\text{ch}}$ ($c \approx 0$), suggesting negligible CME contributions in these collisions. They also confirm that the combined sources of background (LCC, resonances, back-to-back jets, ...), which should be substantial, especially for $p+Pb$, scale as $1/N_{\text{ch}}$. Note as well that the CME contribution is negligible in $p(d)+A$ collisions because of significant reductions in \vec{B} , and the sizable de-correlation between the event plane and the \vec{B} -field [12]. Thus, the scaling patterns of $\Delta\gamma/v_2$ for these

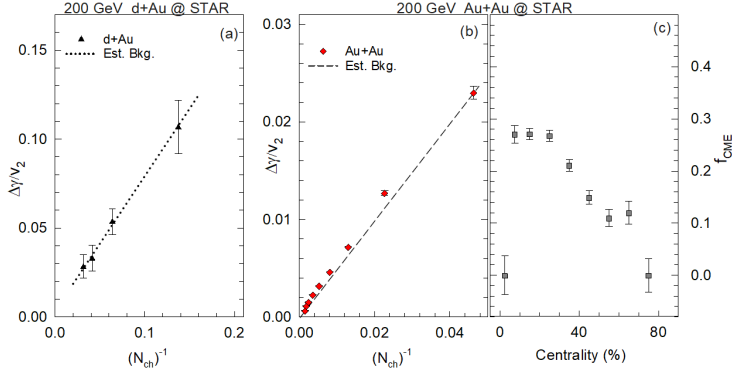


Figure 3. $\Delta\gamma/v_2$ vs. $1/N_{\text{ch}}$ [(a) and (b)] and f_{CME} vs. centrality (c) for $d+\text{Au}$ and $\text{Au}+\text{Au}$ collisions at $\sqrt{s_{\text{NN}}} = 200$ GeV. The dotted and dashed lines indicate an estimate of the background contributions. The data are taken from Refs. [7, 9?].

systems' sizable backgrounds give a direct experimental constraint on the validity of $1/N_{\text{ch}}$ scaling of the background.

The scaling results for collisions at $\sqrt{s_{\text{NN}}} = 200$ GeV are shown in Fig. 3. The $1/N_{\text{ch}}$ scaling apparent for $d+\text{Au}$ collisions (Fig. 3 (a)) confirms the expectation that the CME is negligible in these collisions. It also confirms that the combined sources of background (LCC, resonances, back-to-back jets, ...), which could be substantial in $d+\text{Au}$ collisions, show $1/N_{\text{ch}}$ scaling. In contrast to $d+\text{Au}$, the results for $\text{Au}+\text{Au}$ (Fig. 3(b)) show visible indications of a violation ($c > 0$) to the $1/N_{\text{ch}}$ scaling observed for background-driven charge separation in $p(d)+\text{A}$ collisions. Similar violations were observed for $\text{Ru}+\text{Ru}$ and $\text{Zr}+\text{Zr}$ [17]. The scaling violation is similar to that observed for signal + background in Figs. 1 (a) and (c), suggesting an unambiguous non-negligible CME contribution to the measured $\Delta\gamma/v_2$ in $\text{Au}+\text{Au}$, $\text{Ru}+\text{Ru}$, and $\text{Zr}+\text{Zr}$ collisions. The CME contribution can be quantified via fits with the function $\Delta\gamma/v_2 = a + b/(N_{\text{ch}})^{1-c}$, to evaluate c . Alternatively, estimates of the background for all three systems can be estimated by leveraging the $\Delta\gamma/v_2$ measurements for peripheral and central collisions with $1/N_{\text{ch}}$ scaling [17]. Here, it is important to recall that the simulated results from the AVFD and HIJING models, as well as the measurements presented in Figs. 2 and 3(a), provide strong constraints that the combined sources of background, scale as $1/N_{\text{ch}}$ over the full centrality span. The background estimates were used to extract f_{CME} values for $\text{Au}+\text{Au}$, (Fig. 3 (c)) $\text{Ru}+\text{Ru}$ and $\text{Zr}+\text{Zr}$ collisions respectively. They indicate non-negligible f_{CME} values that vary with centrality. In mid-central collisions, $f_{\text{CME}} \sim 27\%$ for $\text{Au}+\text{Au}$ collisions, which is roughly a factor of two larger than the values for $\text{Ru}+\text{Ru}$ and $\text{Zr}+\text{Zr}$. Within the uncertainties, no significant difference between the values for $\text{Ru}+\text{Ru}$ and $\text{Zr}+\text{Zr}$ was observed, suggesting that $\Delta\gamma/v_2$ is sensitive to CME-driven charge separation in $\text{Ru}+\text{Ru}$ and $\text{Zr}+\text{Zr}$ collisions but may be insensitive to the signal difference between them [17].

In summary, we demonstrate that the scaling properties of the $R_{\Psi_2}(\Delta S)$ and the $\Delta\gamma$ correlators can be used to characterize the CME in colliding systems at RHIC and the LHC. The $\Delta\gamma/v_2$ measurements for $p+\text{Au}$ and $d+\text{Au}$ collisions at $\sqrt{s_{\text{NN}}} = 200$ GeV and $p+\text{Pb}$ ($\sqrt{s_{\text{NN}}} = 5.02$ TeV) and $\text{Pb}+\text{Pb}$ collisions at $\sqrt{s_{\text{NN}}} = 5.02$ and 2.76 TeV, scales as $1/N_{\text{ch}}$ consistent with background-driven charge separation. However, the results for $\text{Au}+\text{Au}$, $\text{Ru}+\text{Ru}$ and $\text{Zr}+\text{Zr}$ collisions ($\sqrt{s_{\text{NN}}} = 200$ GeV) show scaling violations, which indicate a CME-driven contribution in the presence of significant background. In mid-central collisions,

$f_{\text{CME}} \sim 27\%$ for Au+Au collisions and is approximately a factor of two smaller in Ru+Ru and Zr+Zr collisions with similar magnitudes for the two isobars.

References

- [1] D. Kharzeev, Phys. Lett. B **633**, 260-264 (2006)
- [2] M. Asakawa, A. Majumder and B. Muller, Phys. Rev. C **81** (2010), 064912
- [3] S. A. Voloshin, Phys. Rev. C **70** (2004), 057901
- [4] N. Magdy *et al.*, Phys. Rev. C **97** (2018) no.6, 061901
- [5] B. I. Abelev *et al.* [STAR], Phys. Rev. C **81** (2010), 054908
- [6] B. I. Abelev *et al.* [STAR], Phys. Rev. Lett. **103** (2009), 251601
- [7] L. Adamczyk *et al.* [STAR], Phys. Rev. C **88** (2013) no.6, 064911
- [8] L. Adamczyk *et al.* [STAR], Phys. Rev. Lett. **113** (2014), 052302
- [9] J. Adam *et al.* [STAR], Phys. Lett. B **798** (2019), 134975
- [10] M. Abdallah *et al.* [STAR], Phys. Rev. C **105** (2022) no.1, 014901
- [11] B. Abelev *et al.* [ALICE], Phys. Rev. Lett. **110** (2013) no.1, 012301
- [12] V. Khachatryan *et al.* [CMS], Phys. Rev. Lett. **118** (2017) no.12, 122301
- [13] A. M. Sirunyan *et al.* [CMS], Phys. Rev. C **97** (2018) no.4, 044912
- [14] S. Acharya *et al.* [ALICE], Phys. Lett. B **777** (2018), 151-162
- [15] S. Acharya *et al.* [ALICE], JHEP **09** (2020), 160
- [16] R. A. Lacey, N. Magdy, P. Parfenov and A. Taranenko, [arXiv:2203.10029 [nucl-ex]].
- [17] R. A. Lacey and N. Magdy, [arXiv:2206.05773 [nucl-ex]].